# Are Zinc oxide nanoparticles safe? A structural study on human serum albumin using *in vitro* and *in silico* methods

Marziyeh Hassanian, Hassan Aryapour*, Alireza Goudarzi, Masoud Bezi Javan

Department of Biology, Faculty of Science, Golestan University, Gorgan, Iran

*Corresponding author. Department of Biology, Faculty of Science, Golestan University, Gorgan, Iran. e-mail: h.aryapour/at/gu.ac.ir

## Abstract

With due attention to adsorption of proteins on the nanoparticles surface and the formation of nanoparticle-protein corona, investigation of nanoparticles toxicity on the structure of proteins is important. Therefore, this work was done to evaluate toxicity of Zinc oxide nanoparticles (ZnO NPs) on the structure of human serum albumin (HSA) through *in vitro* and *in silico* studies. First, ZnO NPs were synthesized using hydrothermal method and their size and morphology were determined by SEM and TEM methods and then to study its toxicity on the HSA structure were used UV-Vis and fluorescence spectroscopy. In order to interpret experimental results and interactions of ZnO NP with HSA at the atomistic level was used molecular dynamics (md) simulation. The obtained images from SEM and TEM showed that ZnO NPs were nanosheet with size of less than 40 nm. The results of spectroscopic studies showed ZnO NPs lead to significant conformational changes in the protein's absorption and emission spectra. Moreover, md results indicated that the inserting of ZnO NP into simulation box lead to unfolding of HSA at the beginning of simulation and the most important factor in the unfolding of protein structure is the non-covalent electrostatic interactions between polar charge groups of HSA and ZnO NP, even when the nanoparticle is located far away - greater than 4 Å - from the protein.

**Keywords:** Human serum albumin, Zinc oxide nanoparticle (ZnO NP), Molecular dynamics simulation, Toxicity

## 1. Introduction

Nanotechnology is the ability to study and use of particles in dimensions between 1-100 nm which commonly known as nanoparticles (NPs). NPs have unique mechanical and chemical

properties arising from their high surface area and quantum effects. Therefore, NPs are used in a wide range of different applications and humans can be exposed to NPs via several routes such as inhalation, injection, oral ingestion and the dermal route [1]. Upon the entry of NPs into the human body, they may interact with biomacromolecules and even biological metabolites due to their nano size and large surface to mass ratio. But, the adsorption of proteins on the surface of NPs and the formation of nanoparticle-protein complex which is known as the nanoparticle-protein corona (NP-PC), is unique [2]. On the other hand, adsorption of proteins on the NPs surface may result in structural changes and unfolding of proteins and lead to toxicity [3]. The previous studies showed that the binding of ZnO NPs led to the denaturation of the periplasmic domain of ToxR protein of *Vibrio cholerae* [4]. Therefore, it is important to study the toxicity of NPs on the structure of proteins to design nanoparticle that do not have toxic effects on the structure of proteins and consequently, on living organisms. In this study, we synthesized ZnO NPs and studied their toxicity on human serum albumin (HSA). These nanoparticles are an important class of commercially applied material and used in diagnostics, therapeutics, drug delivery systems, electronics, cosmetics, personal care products, food additives and pigments and coatings due to their magnetic, catalytic, semiconducting, antimicrobial, ultraviolet protective and binding properties [5,6]. Moreover, human serum albumin is the most abundant type of plasma protein (3.5 to 5.5 g/dL) with highest electrophoretic mobility, and it has a globular structure with a molecular weight 66.5 kDa, consists of 585 amino acids, 17 disulfide bonds, and only one free thiol group (Cys34) [7]. HSA comprises three homologous domains (I, II, and III) that assemble to form a heart-shape molecule and each domain is divided into two subdomains A and B [8]. The function of HSA is the maintenance of colloid osmotic pressure and transportation, distribution and metabolism of many endogenous and exogenous small molecules and ions [9-11]. Thus, due to the increasing use of ZnO NPs in various products and also the biomedical importance of HSA in human health, we investigated the toxicity of ZnO NPs on the structure of this protein through *in vitro* and *in silico* studies.

## 2. Materials and Methods

### 2.1. Materials

Zinc acetate dihydrates [(Zn $(CH_3COO)_2.2H_2O$)], ti-sodium citrate and sodium hydroxide were purchased from Merck Company and Human serum albumin (96%) and ANS (1-anilino-8-naphthalene sulfonic acid) were purchased from Sigma-Aldrich.

## 2.2. Synthesis of ZnO NPs

ZnO NPs were synthesized using hydrothermal method as follows [12]. First, 60 ml of 1 M Zinc acetate and 30 mL of 0.5 M citrate were mixed in a baker, then 50 mL distilled water and 60 ml of 1 M sodium hydroxide were added dropwise to the mixed solution along with sonication. The obtained white solution was incubated at room temperature for 24 h, and then the resulting pellet was washed with distilled water several times, and lyophilized to give nanopowder. The size and morphology of ZnO NPs were determined by SEM (Hitachi S-4160) and TEM (Philips CM 120).

## 2.3. Spectroscopy procedures

All experiments were performed in 0.1 mM sodium phosphate buffer (pH 7.4), and different concentration of ZnO NPs (0, 0.1, 0.2, 0.3, 0.4 and 0.5 mg/mL) were incubated with a constant concentration of HSA (5 μM) for 1 h at room temperature. The UV-Vis absorption spectra were recorded with double-beam Shimadzu UV-1800 UV-Vis spectrophotometer. After incubation of HSA with different concentrations of ZnO NPs, the absorption spectra were taken in the wavelength range of 200-500 nm. Time kinetics study was done using a BioTek ELx808IU microplate reader at pH 7.4 to determine the time depended absorption of HSA interaction (5 μM) with ZnO NP (0.5 mg/mL) under temperature 37 °C for 120 min.

Also, fluorescence analyses were carried out using a PerkinElmer LS 55 fluorescence spectroscopy and scan speed and excitation slit width were set at 500 and 5 nm, respectively. In intrinsic fluorescence after incubation of HSA with ZnO NPs, fluorescence intensity of tryptophan (Trp) residue was measured in the absence and presence of different concentrations of ZnO NPs. The excitation wavelength was adjusted at 295 nm and emission spectra were recorded in the wavelength range of 300-500 nm, and so the Stern-Volmer equation was used to determine the mechanism of quenching as following [13]:

$$F_0/F = 1 + K_{SV}\,[Q] = 1 + Kq\,\tau_0\,[Q]$$

Where $F_0$ and F are the fluorescence intensity of HSA in the absence and presence of quencher (ZnO NPs), respectively. $K_{SV}$ is the Stern-Volmer quenching constant, [Q] is the concentration of quencher, Kq is the quenching rate constant and $\tau_0$ is the average lifetime of HSA in the absence of quencher and its value is $10^{-8}$ s [14]. In addition to Trp emission, also ANS fluorescence probe was used for monitoring conformational changes in HSA [15]. First, HSA was incubated with ANS (3 μM) and different concentrations of ZnO NPs, and then fluorescence

intensity of ANS was measured in the absence and presence of different concentrations of ZnO NPs in the wavelength range of 400-600 nm, upon excitation at 350 nm.

### 2.4. Theoretical procedures

In order to interpret experimental results and understanding HSA unfolding at the atomistic level in the presence of ZnO NPs, md simulations were carried out using the Amber99SB force field [16], in Gromacs package, version 2018 [17]. The crystallographic structure of holo human serum albumin (PDB ID: 1e7e) was obtained from Protein Data Bank [18]. To understand the mechanism of ZnO NPs effect on HSA structure, theoretical studies were done in several different forms. The simulation systems 1 and 2 include apo-HSA and holo-HSA forms respectively, and they were used as control. While, the simulation systems 3 and 4 includes apo-HSA and holo-HSA forms with ZnO NP, respectively. In holo form, HSA is in complex with ten molecules of deprotonated form of decanoic fatty acid (DKA). The topology parameters of the fatty acid were generated by ACPYPE tool [19]. In the all md simulations was used from a spherical ZnO NP with diameter of 4 nm which has hexagonal wurtzite-type crystal structure with the lattice constants a=3.25 Å and c=5.2 Å [20]. The interactions between Oxygen and Zinc atoms are described by Lennard-Jones potentials and the values of σ and ε parameters respectively are set to 2.128 Å and 0.418 $kJ.mol^{-1}$ for the O atom and 1.711 Å and 1.254 $kJ.mol^{-1}$ for the Zn atom. Partial charges (+1.026 and -1.026 for Zn and O atoms, respectively) were taken from the previous studies [21]. In all simulation, protein and ZnO NP were placed in the center of a triclinic box with a distance of 1 nm from all edges, and under periodic boundary conditions (PBC). The distance between ZnO NP and HSA in the simulation systems 3 and 4 was set to 13 Å. Then simulation boxes were filled by TIP3P water molecules [22] and the systems were neutralized by adding $Na^+$ and $Cl^-$ ions at the physiological concentration of 150 mM. The energy of the systems was minimized using the steepest descent algorithm and the minimization has stopped when the $F_{max}$ was smaller than 10 $kJ.mol^{-1}.nm^{-1}$. Then, 100 ps NVT and 300 ps NPT ensembles were performed for each system until the temperature and pressure of the systems reach stable states in the 310 K and 1 atm, respectively. Also during the simulation was used from Particle Mesh Ewald (PME) method [23] and LINCS [24] and SETTLE [25] algorithms to calculate the long-range electrostatic interactions and constrain the length of bonds and position of the TIP3P water molecules, respectively. The cut-off for the coulomb and van der Waals interactions was set to 1.2 nm. Finally, all the systems were simulated for 200 ns and with time step of 2 fs. Also, in order to investigate the role of disulfide bonds in the stability of HSA

structure in the presence of ZnO NP, the last frame of each simulation system was extracted, and then extended for 50 ns without disulfide bonds. The trajectories analysis was performed using GROMACS utilities and VMD and USCF Chimera [26,27].

## 3. Results and Discussion

### 3.1. Characterization of ZnO NPs

The SEM and TEM images of ZnO NPs are shown in (Figure 1a). The sheet like morphology of the ZnO NPs with approximate thickness less than 40 nm are seen.

### 3.2. UV-Vis spectroscopy and Time kinetics analyses

One of the most effective methods to study the structural changes in proteins is UV-Vis spectroscopy [28]. UV-Vis absorption spectra of HSA in absence and presence of ZnO NPs are shown in (Figure 1b). The absorption spectra for HSA show two peaks at wavelengths of 230 and 280 nm. In order to investigate the conformational changes in the protein we studied the absorption spectra at 280 nm which corresponds to the $\pi$-$\pi^*$ electron transitions of aromatic amino acids (Trp, Tyr and Phe) [29]. The absorption spectra of HSA at 280 nm gradually increased with the increasing of ZnO NPs concentration with no shift in absorption intensity. Similar results were observed in the articles which the ground state complex between proteins and NPs was formed [28,30]. Therefore, this increasing in the absorption intensity can be due to formation of the ground state complex between HSA and ZnO NPs. Also, it is possible that with the increasing of ZnO NPs concentration, it induced the unfolding of HSA and increased exposure of aromatic amino acid which followed with the increasing of adsorption intensity. Also, the time dependent absorption of HSA in the presence of ZnO NPs showed that the reaction between ZnO NPs and HSA, and consequently the conformational changes of HSA structure occur within the first 40 min, and thereafter no appreciable change in the absorption increasing occurs (Figure 1c).

### 3.3. Fluorimetric analyses

Intrinsic or natural fluorescence of proteins originates with the three aromatic amino acid residues include tryptophan, tyrosine and phenylalanine. HSA has only one tryptophan which present in the bottom of hydrophobic pocket in domain IIA (Trp 214). This residue is highly sensitive to its local micro-environment and a trivial change in the local environment either by ligand binding or conformational changes would significantly quench it [10,28]. Phenylalanine has

a very low quantum yield and the fluorescence of tyrosine can be quenched if it's ionized or placed near an amino group, a carboxyl group or a tryptophan [31,32]. For identifying variations in HSA folding, fluorescence emission spectra of tryptophan in absence and presence of ZnO NPs were measured using fluorescence spectroscopy (Figure 1d). The emission intensity of Trp decreases with an increase in ZnO NPs concentration which indicates quenching of the intrinsic HSA fluorescence by ZnO NPs. Previous works have reported similar quenching on the interaction of proteins with NPs [29,32]. The emission intensity maximum of Trp shows a small red shift that suggesting ZnO NPs likely induced structural changes and unfolding in HSA. According to the Stern-Volmer plot (Figure 1e), the plot of F0/F against [Q] is a straight line and slope of line is $K_{SV}$. Therefore, was calculated a value of $2 \times 10^2$ $M^{-1}$ for $K_{SV}$ and using the $\tau_0 = 10^{-8}$ s was calculated $2 \times 10^{10}$ $M^{-1}s^{-1}$ for Kq. To study the extrinsic fluorescence, we used from ANS that is a fluorescent probe and binds to hydrophobic pockets on the surface of proteins, that in HSA, it binds mainly to subdomain IIIA and formed ANS-HSA complex [15,33]. Therefore, the change in the ANS emission spectra gives useful information about conformational change of protein. ANS alone does not show any fluorescence emission, while the binding of it to HSA shows the fluorescence emission intensity gradually increased along the increasing of ZnO NPs concentration (Figure 1f). This indicated that with the increasing of ZnO NPs concentration, occurred unfolding of HSA and exposed hydrophobic pockets of protein that were buried in the interior of HSA molecule, and then the binding of ANS to these pockets along emission intensity increased. Also a slightly blue shift in the maximum emission wavelength could be observed, that suggesting likely the folding of HSA altered in the presence of ZnO NPs.

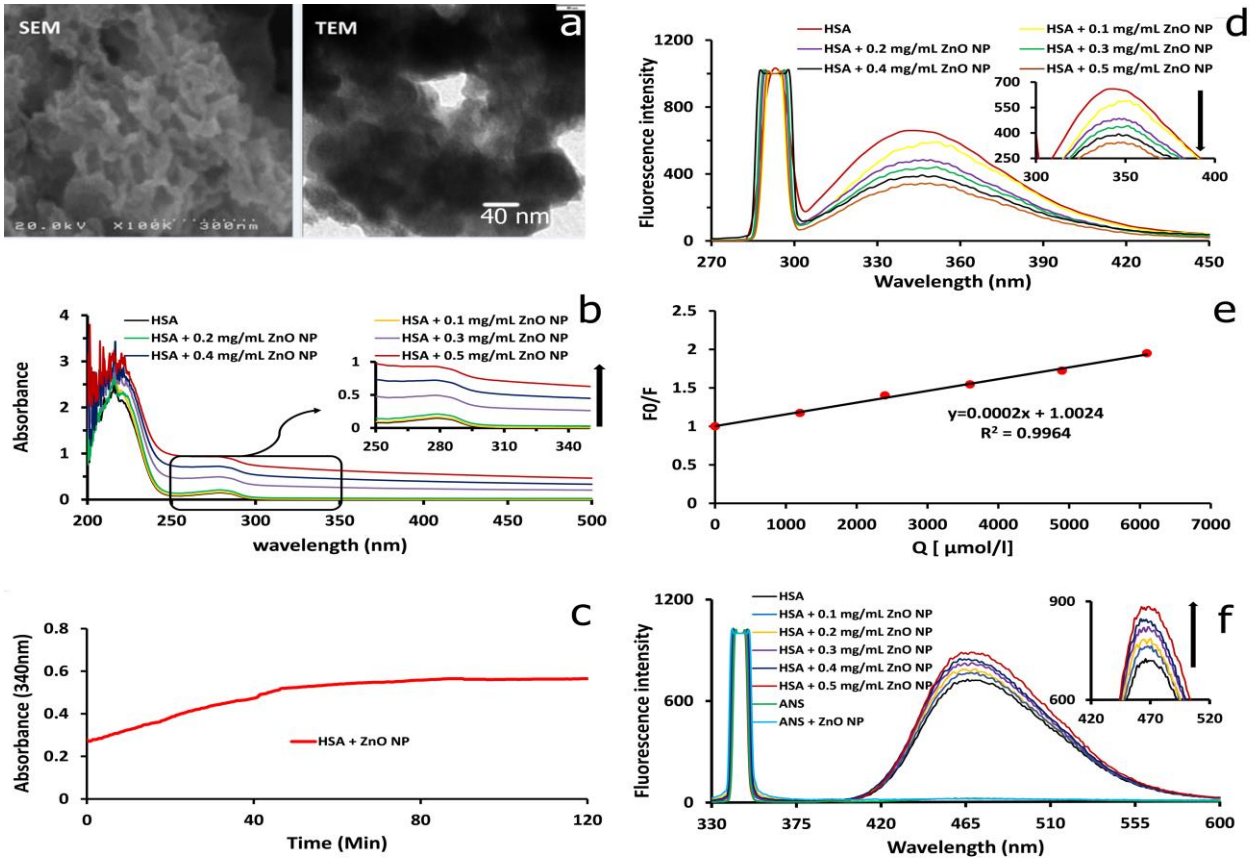


**Figure 1. SEM and TEM micrographs of ZnO NPs (a). UV-Visible spectra of HSA in the presence of different concentrations of ZnO NPs (b). Time kinetics plot of HSA in the presence of 0.5 mg/mL of ZnO NPs (c). Intrinsic fluorescence spectra of HSA in the presence of increasing concentration of ZnO NPs (d). The Stern-Volmer plot of fluorescence quenching of HSA by ZnO NPs (e). Extrinsic fluorescence spectra of HSA in absence and presence of different concentrations of ZnO NPs (f).**

### 3.4. Molecular dynamics simulation analyses

To investigation the stability and dynamics of HSA, we used Root Mean Square Deviation (RMSD) analysis, which show the conformational and orientational changes of the protein structure by comparing the displacement in the position of protein atoms relative to the reference structure [34]. In the absence of the nanoparticle, the RMSD values of holo and apo-HSA remained below 0.3 and 0.4 nm, respectively. Therefore, these forms are rigid and more stable during the 200 ns simulation. But, RMSD values gradually increased to 1.5 and 2.5 nm, respectively, in the presence of the nanoparticle, which indicate interaction of ZnO NP with HSA lead to protein unfolding. Also, because of the presence of fatty acid in the holo-HSA, the RMSD changes are less than apo form. In order to understand the importance of disulfide bridges in the stability of the HSA structure, we removed disulfide bonds from the protein structure in all systems and extended simulations up to 250 ns. The results show that the RMSD values increased, and lead

to more structural instability. Therefore, disulfide bonds play an important role in the HSA stability (Figure 2a).

Also, we used Root Mean Square Fluctuation (RMSF) analysis to obtain the fluctuations and movements of the backbone residues of HSA during simulation. Therefore, the system is stable when the RMSF value is less. The fluctuations of residues of HSA in presence ZnO NP are more due to interaction of ZnO NP with HSA. Moreover, the RMSF value is less in holo-HSA as compared to apo-HSA and is more stable due to the presence of the fatty acids in protein structure and RMSF values of HSA domain III (significantly subdomain IIIB) in all simulation systems is more from domain I and II that show it is more instable during simulation and first gets unfold in the unfolding process (Figure 2b).

To measure the compactness of HSA structure we used Rg analysis that is defined as the approximate distance of atoms from the center of protein. Smaller and larger values of the Rg can be a sign of the folding and unfolding of protein, respectively. The Rg value of HSA in presence ZnO NP is more, that is the reason for protein unfolding (Figure 2c).

During the unfolding of proteins, the amount of solvent accessible surface area (SASA) increases, and it indicates significant burial of proteins apolar surface. The results showed that the SASA in the absence of nanoparticle converged within the simulation time, but in the presence of nanoparticle increased. The increase of SASA indicates that protein unfolding occurred and apolar regions exposed to solvent (Figure 2d). Consequently, in the HSA unfolding effect by ZnO NP, some of the fatty acids in the holo-HSA form are separated from the protein structure.

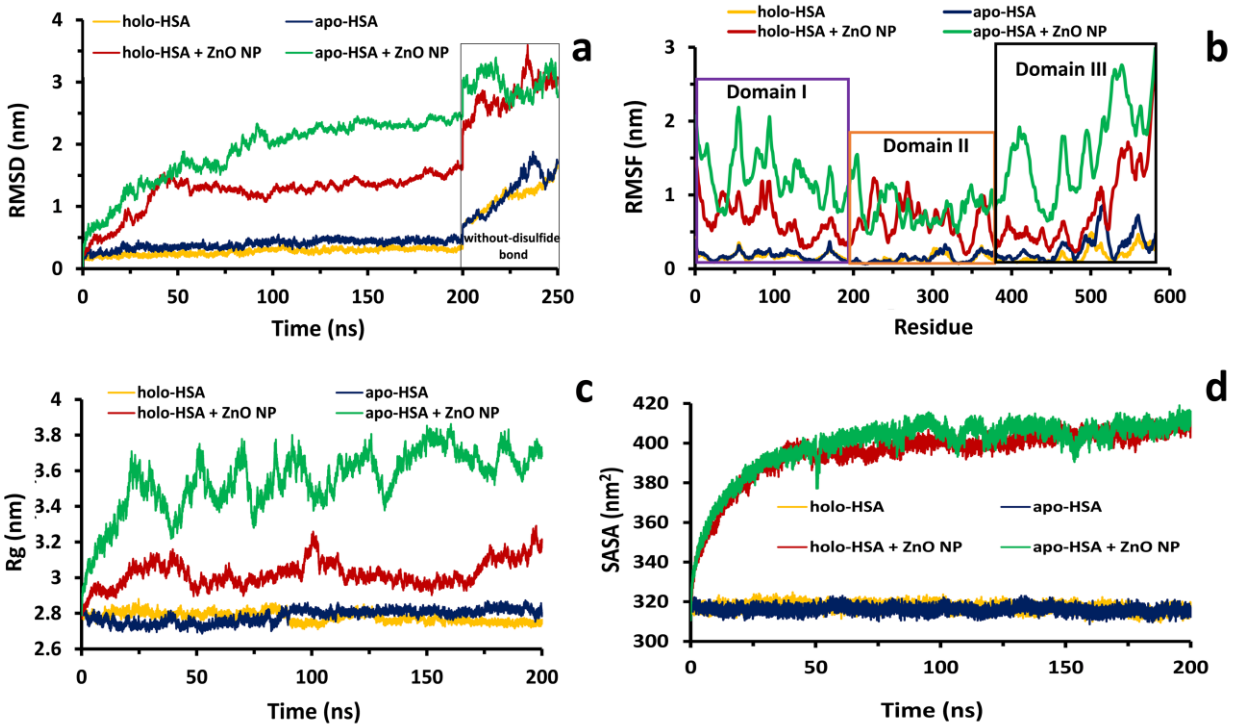


**Figure 2. Backbone RMSD plot of holo- and apo-HSA in the absence and presence of ZnO NP (a). Backbone RMSF plot of HSA at different simulation systems (b). RG plot of HSA backbone at different simulation systems (c) and SASA plot of HSA at different simulation systems during 200 ns simulation (d).**

In order to study the secondary structures of protein, we used from DSSP program. In holo and apo-HSA forms the main structure of the HSA is α-helix. But, due to interaction HSA with ZnO NP reduced the amount of α-helix and increased the amount of coils, which represents the unfolding of HSA structure (Figure 3a, b, c, d and Percentage of changes listed in Table 1). Also, ramachandran plots show the values of phi and psi angles of HSA α-helice are in most favoured regions, but in the presence of nanoparticles the irregular secondary structures increased and these angles lie in other zones (Figure 3e, f, g, h).

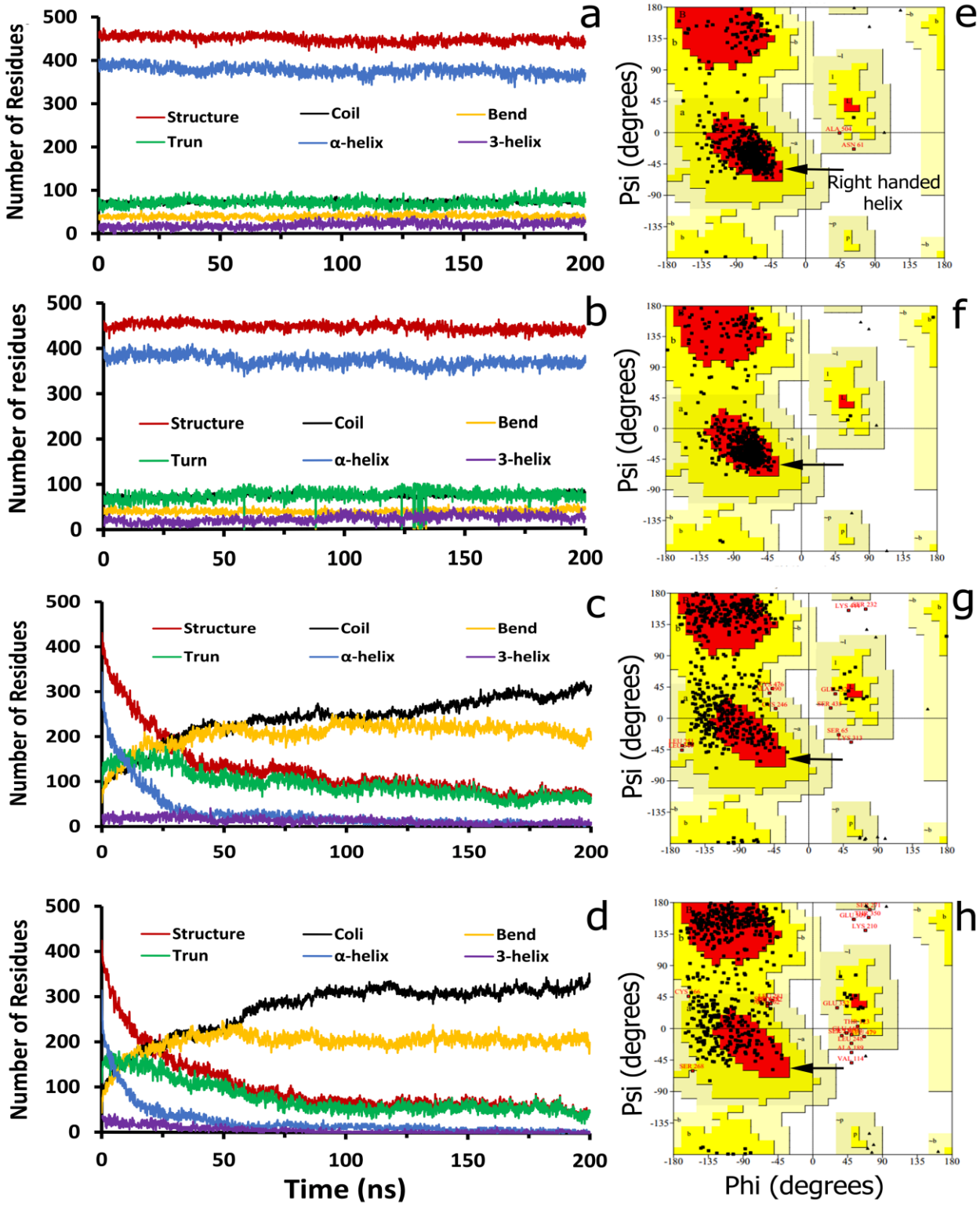


**Figure 3. The secondary structure of holo- (a, c) and apo-HSA (b, d) in the absence and presence of ZnO NP. Ramachandran plot of holo- (e, g) and apo-HSA (f, h) in the absence and presence of ZnO NP.**

**Table 1. The Percentage of HSA secondary structures in different simulation systems during 200 ns**

| Simulation Systems | Structure (α-helix+Turn) | Coil | Bend | Turn | α-helix | 3-helix |
|---|---|---|---|---|---|---|
| **holo-HSA** | **77** | **13** | **7** | 12 | **65** | 3 |
| **holo-HAS + ZnO NP** | **21** | **41** | **35** | 16 | **5** | 2 |
| **apo-HSA** | **77** | **13** | **7** | 13 | **64** | 4 |
| **apo-HAS + ZnO NP** | **17** | **47** | **34** | 13 | **4** | 1 |

Moreover, we investigated hydrogen bonds number of HSA because the stability factor of secondary structures such as α-helix is intrachain hydrogen bonds. In presence of the nanoparticle decreased number of hydrogen bonds, which indicate the loss of helical structures following protein unfolding (Figure 4a).

In addition, we investigated the relationship between conformational changes of HSA with its distance from the surface of nanoparticle. The results showed that the distance between them decreased to less than 0.4 nm and remained constant along simulation time, which indicates electrostatic interactions between Zn and O atoms with acidic and basic residues, respectively. In Figure 4b is shown distance between one of the acidic and basic residues of HSA with Zn and O atoms, respectively. Therefore, electrostatic interactions are the most important factor in the unfolding and adsorption of HSA on the surface of ZnO NPs and the formation of nanoparticle-protein corona (Figure 4c, d).

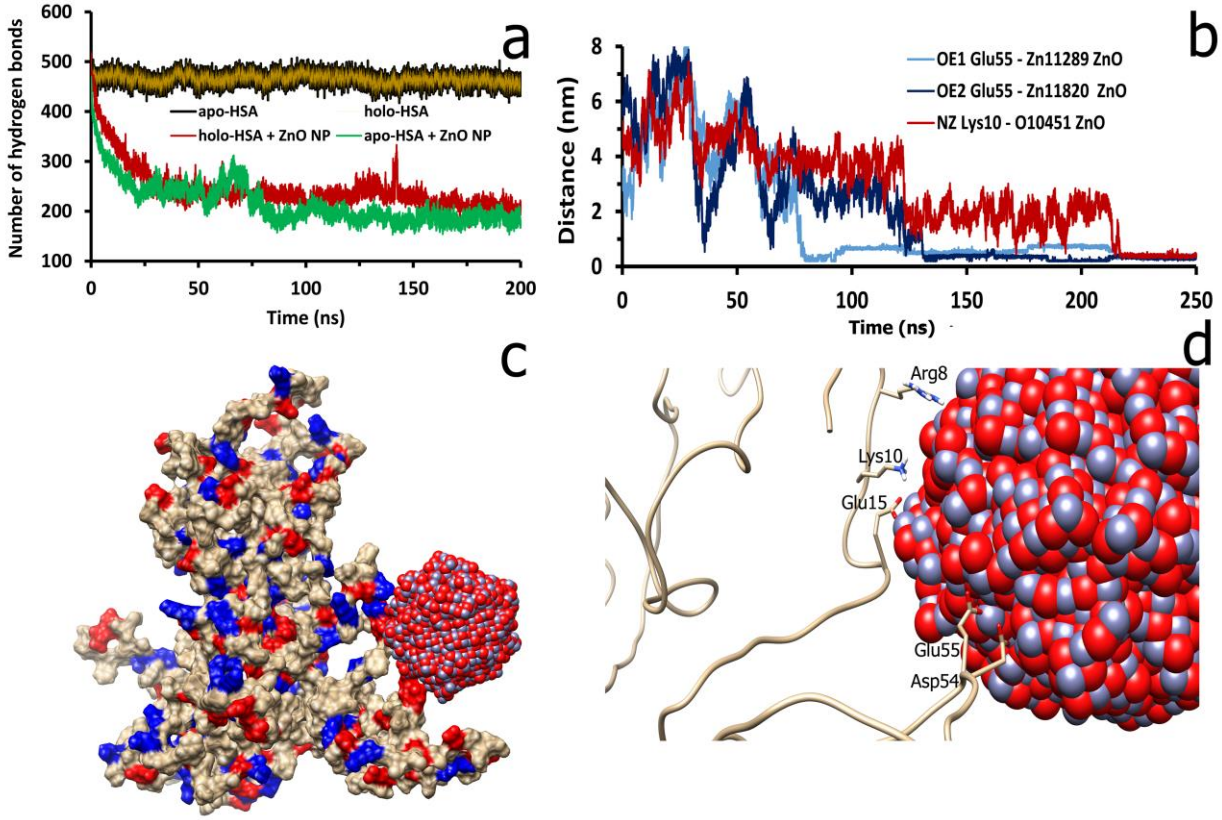


**Figure 4. Number of intrachain hydrogen bonds of HSA at different simulation systems (a). Distance between Glu55 and Lys10 of HSA with Zn and O atoms of ZnO NP respectively, during 250 ns simulation (b). The presentation of non-covalent interactions between HSA and ZnO NP and formation of nanoparticle-protein corona (c, d). Basic and acidic residues of HSA are illustrated as blue and red colors in surface presentation (c) respectively, and other residues are shown in gray.**

Also, we observed HSA unfolding even before the adsorption of HSA on nanoparticle surface. Therefore, it could be concluded that the HSA unfolding in presence ZnO NP is due to abundance of acidic and basic residues in HSA structure - 97 acidic and 83 basic amino acids - and nanoparticle surface charges, and the formation of high attractive and repulsive forces between them (Figure 5).

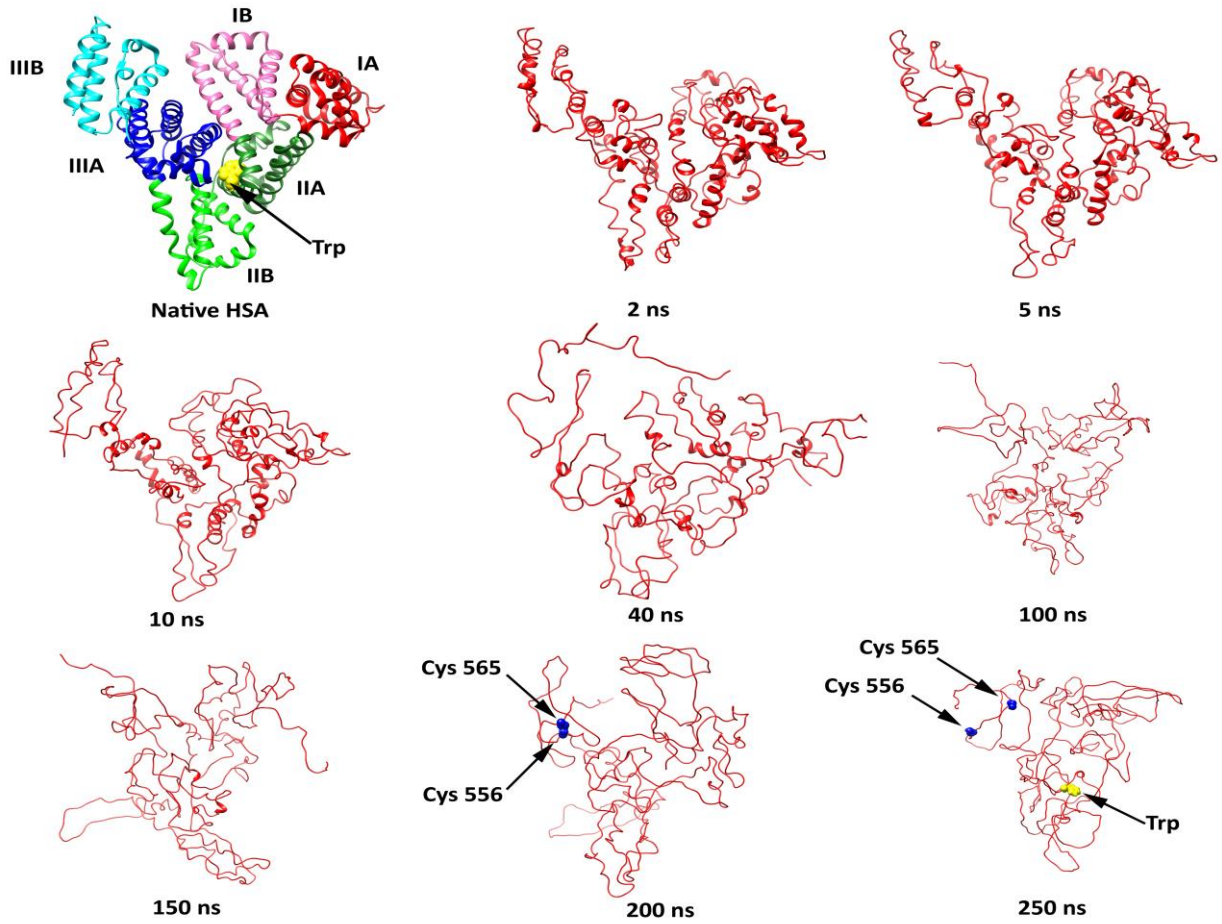


**Figure 5. Snapshots of the conformational changes of apo-HSA structure in the presence of ZnO NP during 250 ns simulation.**

## 4. Conclusion

In the present study, the toxicity of ZnO NPs on HSA was investigated by *in vitro* and *in silico* methods. In *in vitro* studies, the ZnO NPs were synthesized with size less than 40 nm and the morphology of the nanosheet by hydrothermal method. The results of the UV-Vis and fluorescence spectroscopy showed the conformational changes of HSA in presence of ZnO NPs. Also, the Stern-Volmer plot showed that the intrinsic fluorescence of HSA was quenched through static mechanism. Furthermore, the results of md simulation indicated that ZnO NP causes HSA unfolding. So, it can be concluded changes in the absorption and emission spectra, is due to HSA unfolding by ZnO NPs. Also, holo-HSA is more stable compared to apo form because when HSA is in complex with fatty acids due to their hydrophobic and electrostatic interactions with residues, HSA becomes more compact and stable. At the end, we concluded the nature of nanoparticles and proteins have an important role in the adsorption of proteins on

the surface of nanoparticles and toxicity rate of them, and if ZnO NPs enter the body they can have very devastating effects.


## Acknowledgement

This investigation was supported by a grant from Golestan University, Gorgan, Iran.


## Conflict of interest

The authors declare no conflict of interest.

## References


(1) Khanna, P.; Ong, C.; Bay, B. H.; Baeg, G. H. *Nanomaterials (Basel, Switzerland)* **2015**, *5*, 1163.

(2) Saptarshi, S. R.; Duschl, A.; Lopata, A. L. *Journal of nanobiotechnology* **2013**, *11*, 26.

(3) Chakraborti, S.; Joshi, P.; Chakravarty, D.; Shanker, V.; Ansari, Z. A.; Singh, S. P.; Chakrabarti, P. *Langmuir : the ACS journal of surfaces and colloids* **2012**, *28*, 11142.

(4) Chatterjee, T.; Chakraborti, S.; Joshi, P.; Singh, S. P.; Gupta, V.; Chakrabarti, P. *The FEBS journal* **2010**, *277*, 4184.

(5) Vandebriel, R. J.; De Jong, W. H. *Nanotechnology, science and applications* **2012**, *5*, 61.

(6) Choi, S. J.; Choy, J. H. *International journal of nanomedicine* **2014**, *9 Suppl 2*, 261.

(7) Raoufinia, R.; Mota, A.; Keyhanvar, N.; Safari, F.; Shamekhi, S.; Abdolalizadeh, J. *Advanced pharmaceutical bulletin* **2016**, *6*, 495.

(8) Nerusu, A.; Reddy, P. S.; Ramachary, D. B.; Subramanyam, R. *ACS omega* **2017**, *2*, 6514.

(9) Artali, R.; Bombieri, G.; Calabi, L.; Del Pra, A. *Farmaco (Societa chimica italiana : 1989)* **2005**, *60*, 485.

(10) Sen, T.; Mandal, S.; Haldar, S.; Chattopadhyay, K.; Patra, A. *The Journal of Physical Chemistry C* **2011**, *115*, 24037.

(11) Ang, J. C.; Henderson, M. J.; Campbell, R. A.; Lin, J. M.; Yaron, P. N.; Nelson, A.; Faunce, T.; White, J. W. *Physical chemistry chemical physics : PCCP* **2014**, *16*, 10157.

(12) Wang, Y.; Ma, Q.; Jia, H.; Wang, Z. *Ceramics International* **2016**, *42*, 10751.

(13) Dadras, A.; Riazi, G. H.; Afrasiabi, A.; Naghshineh, A.; Ghalandari, B.; Mokhtari, F. *JBIC Journal of Biological Inorganic Chemistry* **2013**, *18*, 357.

(14) Huang, H.; Liu, X.; Han, R.; Wang, G. *J Environ Anal Chem* **2017**, *4*, 2380.

(15) Aghili, Z.; Taheri, S.; Zeinabad, H. A.; Pishkar, L.; Saboury, A. A.; Rahimi, A.; Falahati, M. *PloS one* **2016**, *11*, e0164878.

(16) Hornak, V.; Abel, R.; Okur, A.; Strockbine, B.; Roitberg, A.; Simmerling, C. *Proteins* **2006**, *65*, 712.

(17) Abraham, M. J.; Murtola, T.; Schulz, R.; Páll, S.; Smith, J. C.; Hess, B.; Lindahl, E. *SoftwareX* **2015**, *1-2*, 19.

(18) Bhattacharya, A. A.; Grune, T.; Curry, S. *Journal of molecular biology* **2000**, *303*, 721.

(19) Sousa da Silva, A. W.; Vranken, W. F. *BMC Res Notes* **2012**, *5*, 367.

(20) Nawrocki, G.; Cieplak, M. *Physical chemistry chemical physics : PCCP* **2013**, *15*, 13628.

(21) Hosseinzadeh, G.; Maghari, A.; Farnia, S. M. F.; Moosavi-Movahedi, A. A. Journal *of biomolecular structure & dynamics* **2017**, 1.

(22) Jorgensen, W. L.; Chandrasekhar, J.; Madura, J. D.; Impey, R. W.; Klein, M. L. *The Journal of chemical physics* **1983**, *79*, 926.

(23) Essmann, U.; Perera, L.; Berkowitz, M. L.; Darden, T.; Lee, H.; Pedersen, L. G. *The Journal of chemical physics* **1995**, *103*, 8577.

(24) Hess, B.; Bekker, H.; Berendsen, H. J.; Fraaije, J. G. *Journal of computational chemistry* **1997**, *18*, 1463.
(25) Miyamoto, S.; Kollman, P. A. *Journal of computational chemistry* **1992**, *13*, 952.
(26) Humphrey, W.; Dalke, A.; Schulten, K. *Journal of Molecular Graphics* **1996**, *14*, 33.
(27) Pettersen, E. F.; Goddard, T. D.; Huang, C. C.; Couch, G. S.; Greenblatt, D. M.; Meng, E. C.; Ferrin, T. E. *J Comput Chem* **2004**, *25*, 1605.
(28) Khan, M. J.; Maskat, M. Y. *Int J Pharm Pharm Sci* **2014**, *6*, 43.
(29) Baral, A.; Satish, L.; Das, D. P.; Sahoo, H.; Ghosh, M. K. *New Journal of Chemistry* **2017**, *41*, 8130.
(30) Bhunia, A. K.; Kamilya, T.; Saha, S. *ChemistrySelect* **2016**, *1*, 2872.
(31) Zhang, Y.-Z.; Zhou, B.; Liu, Y.-X.; Zhou, C.-X.; Ding, X.-L.; Liu, Y. *Journal of fluorescence* **2008**, *18*, 109.
(32) Fan, H.; Ji, N.; Zhao, M.; Xiong, L.; Sun, Q. *International journal of biological macromolecules* **2015**, *78*, 333.
(33) Chatterjee, T.; Pal, A.; Dey, S.; Chatterjee, B. K.; Chakrabarti, P. *PloS one* **2012**, *7*, e37468.
(34) Castellanos, M. M.; Colina, C. M. *The journal of physical chemistry. B* **2013**, *117*, 11895.